This is the author's version of an article published in IET Renewable Power Generation. Changes were made to this version by the publisher prior to publication.
DOI: 10.1049/iet-rpg.2014.0345

Transient Stability Enhancement of a Grid-Connected Wind Farm using an Adaptive Neuro-Fuzzy Controlled-Flywheel Energy Storage System

[1]T.A. Taj, [2]Hany M. Hasanien, [1]A. I. Alolah, and [3]S.M. Muyeen

[1]Electrical Engineering Department, College of Engineering, King Saud University, 11421, Riyadh, Saudi Arabia. (e-mail: ttaj@ksu.edu.sa)
[2]Electrical Power and Machines Department, Faculty of Engineering, Ain Shams University, Cairo 11517, Egypt. Also, He is with the Electrical Engineering Department, College of Engineering, King Saud University, Riyadh 11421, S.A. (e-mail: hanyhasanien@ieee.org)

[3]Department of Electrical Engineering, The Petroleum Institute, Abu Dhabi 2533, U.A.E.

***Abstract*— With the rapid growth of the wind energy systems in the past years and their interconnection with the existing power system network, it has become very significant to analyze and enhance the transient stability of the wind energy conversion systems connected to the grid. This paper investigates the transient stability enhancement of a grid-connected wind farm using doubly-fed induction machine (DFIM) based flywheel energy storage system (FESS). A cascaded adaptive neuro-fuzzy based controlling technique is introduced to control the insulated gate bipolar transistor (IGBT) based frequency converter to enhance the transient stability of the wind farm connected to the grid. The performance of the presented control strategy is analyzed under a severe symmetrical fault condition on a single machine infinite bus model and on the IEEE 39-bus New England test system. The transient performance of the system is investigated by comparing the performance of the system using classical PI-controllers and the adaptive neuro fuzzy controllers. The validity of the system is verified by the simulation results which are carried out using PSCAD/EMTDC.**

***Index Terms*—Adaptive neuro-fuzzy controller, doubly fed induction machine, flywheel energy storage system, frequency converter, wind farm.**

I. INTRODUCTION

ALONG with the conventional energy sources, the penetration of renewable energy is increasing day by day. There are several renewable energy sources like solar, wind, biogas and tidal which are getting popular and more investment is now being done in the renewable energy sector. Among these resources, wind energy is considered as one of the most important means of renewable power generation and has an enormous potential to play a vital role in the energy market. The wind energy generated across the world has grown at a rate of more than 30% over the past decade. As per recent statistics cumulative global capacity has reached to a total of 318 GW, which shows an increase of nearly 200 GW in the past five years. It is expected that the wind energy will reach to 600GW by 2018 [1]-[2]. Due to the rapidly increasing wind energy integration into the power system networks, one of the major problems related to transient stability of wind farms is a major concern for the researchers [3]. Nowadays, the integration of different types of energy storage systems (ESS) is used to improve the stability of electrical power systems such as energy capacitor storage (ECS) systems, superconducting magnetic energy storage systems (SMES), battery energy storage systems (BESS), and flywheel energy storage systems (FESS) [4]-[7].

Every ESS has some advantages and disadvantages associated with it. The ECS has some great advantages like extensive operating temperature range, less cost and environmental benefits [8]. Moreover, its low storage capacity and depletion of stored energy over a span of time is a huge disadvantage as compared to the other ESS. On the other hand, fast response and ample storage capacity [9] are some of the advantages of SMES. The major disadvantage of SMES is its high cost. BESS has slow response, since fast charging and discharging capability is required for an ESS; hence, BESS is not an appropriate choice [10]. Also, smaller life time and limited voltage and current are some of the other drawbacks of BESS [11]. Comparing FESS with ECS, SMES and BESS, the FESS has many advantages over other ESS. Its high power density, no harmful chemicals, robustness, longer life span and low maintenance cost are important advantages over other energy storage systems [12-16]. Recent trend of using HTS material is making the FESS system more efficient. Because of these advantages, FESS is increasingly used to improve the stability of the electrical power systems.

The FESS stores the energy in the flywheel (rotor) of the DFIM. The rotational energy is supplied during the fault conditions by continuous exchange of power from the grid. The DFIM is connected to back-to-back

voltage source converters (VSC). First one is the grid side converter (GSC) and the other is rotor side converter (RSC). The VSC consists of 6 back to back insulated gate bipolar transistors (IGBTs) [17]. The gate signals of the IGBTs controls the power flow of the FESS. Moreover, another advantage of the DFIM based FESS is that it can also works as a reactive power compensator [18]. Also, the DFIM requires a small capacity power converter.

The DFIM based FESS can improve the power system stability of wind generator systems [19]. In many studies, the proportional-integral (PI) controllers are considered as a great choice for being used to control the power flow of the FESS between the wind farm and the DFIM during fault conditions efficiently [20]. The PI controller is the most commonly used in the industry due to its robustness and offering wide stability margins. But its major drawback is that the PI controller is highly sensitivity to the parameter variations and nonlinearity of the systems.

This paper presents the transient stability enhancement of a grid connected wind farm using a DFIM based FESS. A novel cascaded adaptive neuro-fuzzy control based FESS model is proposed in this study to enhance the transient stability of the grid connected wind farm. The adaptive controller is applied to two different systems. Firstly, a simple model system is considered in which the wind power generator is connected to an infinite bus through transmission lines. Secondly, the proposed model of the FESS is applied to the IEEE-39 Bus New England Test System. The results of the adaptive neuro-fuzzy controller are compared with that of the PI controller. Simulation results are investigated thoroughly. The validity of the proposed model is verified through simulation using the standard dynamic power system simulator PSCAD/EMTDC [21].

The organization of the paper is given as follows. In Section II, the wind turbine modeling is explained. Section III describes the FESS configuration. In Section IV, proposed control scheme is presented along with the description of the adaptive neuro-fuzzy controller. Simulation results for single machine system are explained in Section V. Section VI describes the IEEE-39 Bus New England test system in detail. Simulation results for the IEEE-39 bus system are presented in Section VII. Section VIII concludes the paper. Section IX is the Appendix.

II. MODEL SYSTEM (SINGLE MACHINE)

The wind farm consists of an aggregated model having five induction generators (IG) each of 2MVA. The wind farm produces 10 MVA. It is connected to the grid through transformers and transmission

lines. The FESS based on DFIM is connected to the wind farm at the point of common coupling (PCC). The single machine infinite bus model system is shown in Fig.1. Table I represents the parameters of the IG and the FESS respectively.

A. Wind Turbine Modelling

The mechanical power produced by the wind turbine is expressed as [22]-[24];

$$P_w = \frac{1}{2}\rho\pi R^2 V_w^3 C_P(\lambda,\beta) \qquad (1)$$

where, P_w is the extracted power from the wind, ρ is the air density [kg/m^3], R is the blade radius [m], V_w is the wind speed [m/s], and C_p is the power coefficient which is a function of tip speed ratio, λ, and blade pitch angle, β[deg.]. In this paper, C_p can be written as follows [25].

$$\lambda = \frac{\omega_m R}{V_w} \qquad (2)$$

$$C_P(\lambda,\beta) = \frac{1}{2}(\lambda - 0.022\beta^2 - 5.6)e^{-0.17\lambda} \qquad (3)$$

where, ω_m is the blade angular velocity [rad/s]. Fig. 2 shows the C_p-λ characteristics for different values of angle β.

B. Modelling of Doubly Fed Induction Machine

The DFIM can be modelled by the following equations [26] in the direct (d) and quadrature (q) axis reference frame, which is rotating at synchronous speed.

Stator voltage and rotor voltage:

$$U_{sd} = -R_s i_{sd} - \rho\phi_{sd} + \omega\phi_{sq} \qquad (4)$$

$$U_{sq} = -R_s i_{sq} - \rho\phi_{sq} + \omega\phi_{sd} \qquad (5)$$

$$U_{rd} = -R_r i_{rd} - \rho\phi_{rd} + \omega\phi_{rq} \qquad (6)$$

$$U_{rq} = -R_r i_{rq} - \rho\phi_{rq} + \omega\phi_{rd} \qquad (7)$$

Stator and rotor flux are represented as;

$$\phi_{sd} = L_s i_{sd} - L_m i_{rd} \qquad (8)$$

$$\phi_{sq} = L_s i_{sq} - L_m i_{rq} \quad (9)$$

$$\phi_{rd} = L_s i_{rd} - L_m i_{sd} \quad (10)$$

$$\phi_{rq} = L_s i_{rq} - L_m i_{sq} \quad (11)$$

The stator power is;

$$P_s = U_{sd} i_{sd} + U_{sq} i_{sq} \quad (12)$$

$$Q_s = U_{sq} i_{sd} - U_{sd} i_{sq} \quad (13)$$

Rotor swing equation is;

$$T_m - T_e = -T_e = \frac{J}{n_P} \frac{d\omega_r}{dt} + \frac{D}{n_P} \omega_r \quad (14)$$

where, U is the voltage, R is the resistance, i is the current, L is reactance, ψ is the flux linkage. d and q represents the direct and quadrature axes components, D is the damping torque, T_m is mechanical torque, n_P and J are considered as number of pole pairs and rotor inertia respectively. And s, r and m indicate stator, rotor and mutual quantities respectively. Fig. 3 represents the DFIM based FESS and its control strategy.

III. FESS CONFIGURATION

The stator windings of the DFIM is coupled with the grid directly while the rotor windings is connected with the VSC. Fig. 3 shows the connection of FESS, it can be seen that the RSC is connected with the rotor side. Both the GSC and RSC are interconnected via high voltage dc link capacitor. The GSC controls the dc link voltage (E_{dc}) and the reactive power (Q_{gen}) while the active power (P_{gen}) of the generator and the wind farm voltage (V_{wf}) are controlled by the RSC. DC link capacitor is interconnecting both GSC and RSC and also ensures the stability of dc link. The GSC converts the DC to AC and supplies the power to the grid.

The carrier frequency of the reference triangular wave is chosen to be 2 kHz. The dc-link voltage across the 2000 μF dc-link capacitor is to be maintained at 4 kV.

IV. PROPOSED CONTROL SCHEME

The control of both GSC and RSC is performed through cascaded adaptive neuro-fuzzy controllers. The reactive power supplied to the grid is controlled through the GSC. It also keeps the dc-link voltage at 4 kV. There are two set of cascaded adaptive neuro-fuzzy controllers for GSC to control the desired variables.

Every controller is segmented into two parts the adaptive neural networks and the fuzzy logic system. A total of 4 cascaded adaptive neuro fuzzy controllers are used to control the FESS. The input of the first cascaded controller is the reference dc-link voltage (4 kV) and the actual value across the dc-link capacitor. The previous output signal from the ANN acts as the third input for the controller. The output of adaptive neural network is fed into the FLC. Now, the signal generated by FLC and the d-axis current (I_d) are fed into the next stage of the cascaded adaptive neuro-fuzzy controller. Similarly, the controlling of the reactive power supplied to the grid works on the same technique. First, the reference and actual reactive power is sent to the adaptive neuro-fuzzy controller which generates an output. The output along with the q-axis current (I_q) are fed to the 2nd stage of the cascaded controller respectively. Also, the active power of the grid and voltage of the wind farm for the RSC are controlled through the adaptive neuro-fuzzy controller in this manner. The RSC is designed to keep the active power and voltage of the wind farm at 1 p.u. The controlling strategy is based on two set of cascaded adaptive neuro-fuzzy controllers each for active power of the wind farm and voltage of the wind farm. The first set of the cascaded controllers is fed by the reference active power along with the actual active power. The signal is fed to the adaptive neural network whose output acts as an input for the fuzzy controller.

The output of the fuzzy controller and the direct-axis current of rotor side (I_{dr}) are sent to the next controller connected in series. Similarly, the cascaded adaptive neuro-fuzzy controller for the voltage of the wind farm works on the same topology described previously. Moreover, the output of the 4 sets of cascaded adaptive neuro fuzzy controllers V_d , V_q, V_{dr} and V_{qr} are transformed from dq0 to abc frame. Fig. 4(a) shows the block diagram representation of the cascaded control for GSC and RSC. The transformed voltages are compared with a triangular waveform with a frequency of 2 kHz. The signals generated from the comparison act as controlling signals for the IGBTs. ANN and FLC details are given in the following sections.

A. ADAPTIVE NEURAL NETWORKS (ANN)

Traditional control theory has some limitations. The assumptions such as linearity and time-invariance has confined the application of classical control theory on non-linear systems [27]. Usually, the conventional PI controller have been used in the control systems because of their wide stability margins and robustness. However, the PI controllers have some limitations, they are highly sensitive to parameters

variation and non-linearity of dynamic systems [27]. Especially for modern non-linear power system applications, tuning the parameters of PI controllers is time consuming and taxing.

Therefore, the problems associated with the conventional PI and PID controllers can be solved by using controllers based on advanced artificial intelligence control techniques. Moreover, the benefit of using these controllers is that they can be applied to the non-linear systems. Also, these controllers are less sensitive to parameter variation as compared to the conventional controllers based on classical control theory [28]. Among many advanced controllers, adaptive neural network (ANN) methods are being used on non-linear electrical power systems. ANN controllers are based on codes inspired from the behavior of neural systems of living beings.

ANNs are based on neurons. There are many topologies for interconnecting of neurons. In this study, the feed forward strategy is used for the interconnection of neurons. There are three inputs of the ANN controller which consist of reference *ref(t)*, actual measured value *actval(t)* and the earlier output signal of the ANN controller *y(t-1)*.

An ANN structure with three neurons in input layer, three neurons in hidden layer, and one neuron in output layer i.e. 3×3×1 structure is shown in Fig. 4(b). The output of a single neuron can be represented by the following equation [3];

$$a_i = f_i\left(\sum_{j=1}^{n} w_{ij} x_j(t) + b_i\right) \quad (15)$$

where, f_i is the activation function, w_{ij} is the weighting factor,

x_j is the input signal, and b_i is the bias.

An activation function is applied on the hidden and output layers of the ANN controller. Nonlinear continuously varying types between two asymptotic values, namely, -1 and +1 are the most commonly utilized activation functions. These functions are known as tansigmoid functions.

The adaptive ANN controller that is implemented in this study is based on the WidrowHoff adaptation algorithm. The Widrow-Hoff delta rule can be used to adapt the Adaline's weight vector [29]-[31]. The weight update equation for the original form of the algorithm can be written as [3]:

$$W(t+1)=W(t)+\alpha.\frac{e(t).x(t)}{|x(t)|^2} \quad (16)$$

where, *W(t+1)*is the next value of the weight vector, *W(t)* is the present value of the weight vector, and *x(t)* is the present input vector.

It can seen from eq. 16 as the weights are changing, the error is reduced by the factor α. The process continuous until the error is reduced to the minimum bounds or becomes zero.

B. *FUZZY LOGIC CONTROLLER (FLC)*

FLCs are advanced controllers and has number of applications. FLC have been applied to many modern control systems which includes the controlling of wind power generators and motors [32]-[34]. FLC has number of design parameters which gives great flexibility for the designer to make an effective controller for the required system. The parameters includes, number of membership functions for each fuzzy input which can be decided as per the complexity of the system, the number of rules, the antecedents and consequents of each rule and the output defuzzification method [35].

The fuzzy system structure has three basic blocks which includes fuzzification, fuzzy interference engine, and the defuzzification. First the fuzzy inputs (crisp inputs) are sent to the fuzzification block where they are fuzzified using the membership functions of the input. Then, the fuzzy interference engine gives a fuzzy sets utilizing the rule base defined by the designer according to the needs of the system to be controlled. Lastly, the defuzzification is applied on the fuzzy sets produced by the fuzzy interference engine. The defuzzification block converts the fuzzy set into a numerical value.

In the system under study, the FLC is used with an ANN. The ANN is connected in series with the FLC making an adaptive neuro fuzzy controller.

The FLC, has two inputs that is the error and change in the input error respectively. In this paper, a 7x7 FLC is implemented. Each input variable has 7 fuzzy sets or membership functions. Similarly, the output is defuzzified using 7 membership functions. The membership functions can be written as;

[NL, NM, NS, Z, PS, PM, PL]

where, NL= negative large, NM=negative medium, NS= negative small, Z=zero, PS= positive small, PM= positive medium, PL= positive large [35].

The membership functions are equally distributed for positive and negative values. Table II contains the 49 rules for the 7x7 FLC.

V. SIMULATION RESULTS FOR SINGLE MACHINE SYSTEM

Modeling of the system and its control strategies are presented in detail. The simulation of the model under study and its transient stability analysis is performed through PSCAD/EMTDC [21]. The wind speed is constant at the rated value of 11.8m/s. The simulation time is 15 s and the solution time step is 20 μs. To study the transient stability of the system, a severe three-line to ground (3LG) fault is applied to point F as shown in Fig. 1. The fault duration is 0.1 s. The results of the system without the FESS is shown in Fig. 5(a) to (e). The system under study is analyzed through PI controlled FESS whose parameters are selected by Black-box optimization technique [36]. The comparison of transient response of the system with adaptive neuro fuzzy controller and PI controller is presented in Fig. 6(a) to (g). It can be noted that the results obtained from the adaptive neuro-fuzzy controller are better than results using the conventional PI-controller. During the fault period, the FESS compensates the active power of the wind farm immediately. The active and reactive power returns back to the reference value as shown in Fig. 6(a) and (b). It can be noted that the response for active and reactive power of the wind farm with adaptive neuro fuzzy controlled FESS is better and have less oscillations than the PI controller controlled FESS. As the fault happens, the IG and turbine speed keep on increasing and becomes unstable when the system is analyzed without FESS as shown in Fig. 5(c) and (d). Moreover, the IG speed and turbine speed has less oscillations and lower settling time with the adaptive neuro fuzzy controlled FESS as shown in Fig 6(c) and (d). The voltage of the wind farm also regains the reference value effectively in the case of adaptive neuro fuzzy controller as shown in Fig. 6(e). Fig 6(f) shows the DC-link voltage. The power of the FESS in Fig. 6(g) shows the continuous exchange of active power between the system and the FESS during the fault and post-fault period. The power of the FESS is zero during the pre-fault period and it again goes back to zero as the system gets stable.

The simulation results prove that the wind turbine IG system become stable using both adaptive neuro-fuzzy controlled and PI-controlled FESS. Moreover, all the system responses using adaptive neuro-fuzzy controlled FESS are better than that of using PI-controlled FESS. Therefore, adaptive neuro-fuzzy controlled FESS is considered to be an effective means for enhancing the transient stability of the wind turbine IG systems.

VI. IEEE 39 BUS NEW ENGLAND TEST SYSTEM

The IEEE 39 bus system also known as 10-machine New England Power System is the compact version of the original New England System. The purpose of this reduced system is to study and analyze new research and advancements on a large and practical electrical power system. Single line diagram of the system is shown in Fig. 7 [37]. The IEEE 39 bus system contains 39 buses out of which 19 are load buses. There are 10 generators in the system. Bus 31 which has generator 2 is defined to be slack bus. The total load and generation in the system is 6150.1 MW and 6192.84 MW respectively. The load model is considered to be constant current (I) and constant admittance (Y) load [37]. The power flow data and dynamics data of the models used are presented in the following sections

After testing the proposed FESS on a single machine infinite bus system, the controller is also applied to the IEEE-39 bus system. The power generation for the 10 generates varies from 250MW to 1000MW. In order to test the proposed FESS with the IEEE-39 bus system, Generator 10 connected at bus 30 which is producing 250MW is replaced by the wind power generator which is connected to the FESS at the PCC. The data corresponding to these generators are given in Table III in Appendix. Table IV contains the bus data. Table V has the IEEE-39 bus load data. All the parameters for the IEEE-39 bus system are given in Appendix [38].

VII. SIMULATION RESULTS FOR IEEE-39 BUS SYSTEM

The IEEE-39 bus system is presented in this study. The coupling of the New England system with the proposed model is investigated. The transient stability analysis is performed through PSCAD/EMTDC. The simulation time is 15 s and the solution time step is 20 μs. Moreover, the wind speed is kept constant at the rated value of 11.8m/s. To ensure and validate the effectiveness of the proposed system and its control strategy a severe 3LG is applied for a duration of 0.1s on bus 30 of the IEEE 39 bus system as shown in Fig. 7.

The system is analyzed for three cases. First, the response of the system without FESS is investigated. Then, the system response with a PI controlled FESS is analyzed and lastly, the simulation results using adaptive neuro fuzzy controlled FESS are investigated and compared with that of the PI controller. Without the FESS system, the active and reactive power of the wind farm becomes unstable and fluctuates heavily as the fault happens. Also, after the fault, the turbine speed and the induction generator speed keep on increasing which makes the system unstable. As a result of the increasing speed of the IG and turbine, the voltage of the wind

farm oscillates. So, it is clear that the system without FESS is highly unstable. Therefore, in order to achieve the transient stability, the system is tested with FESS having two different control strategies.

First, the PI controlled FESS is connected with the system. The parameters of the PI controller are selected using the Black-box optimization technique.

As the fault happens, the FESS compensates the active and reactive power of the wind farm by continuously exchanging the power through flywheel. Fig. 8 (a) and (b) shows the active and reactive power of the wind farm. It can be noted that the adaptive neuro fuzzy controller has response and less over shoot than the FESS with PI controller. Moreover, the IG speed and the turbine speed comes back to the pre-fault values using both the PI and the adaptive neuro fuzzy controller but the response of the adaptive controller is notably better than that of a PI controller as shown in Fig. 8 (c) and (d). Similarly, Fig. 8 (e) and (f) shows the voltage of the wind farm and the dc link voltage. The Power of the FESS can be seen in Fig. 8 (g), which shows better exchange of power in the case of adaptive neuro fuzzy controller.

Comparing the results of the PI controlled FESS with the adaptive neuro fuzzy controlled based FESS, it is evident that the adaptive controller performs better and gives more precise and efficient result as compared to the classical PI-controller.

The results prove that the wind turbine system coupled with the IEEE 39 bus New England test system becomes stable and performs appropriately with both the PI controlled FESS and the adaptive neuro-fuzzy controlled FESS. Moreover, it is to be stated that the response of the proposed system is much better with adaptive controlled FESS as compared to the PI controlled FESS.

VIII. CONCLUSION

This paper has introduced a novel adaptive neuro-fuzzy controlled FESS to enhance the transient stability of a grid-connected wind generator system. Detailed modeling and control strategies of the system under study are presented. The results has shown that the integration of a PI or an adaptive neuro-fuzzy controlled FESS with the wind generator system results in obtaining a stable system when a severe 3LG fault is applied. The transient response of the system with adaptive neuro-fuzzy controlled FESS is much better than that obtained with PI-controlled FESS. The proposed model performed efficiently and effectively on a single machine infinite bus system. The proposed model has also been applied to the IEEE-39 bus New England test system. The results were better and the transient stability of the system improved notably as compared to the system

without FESS. Therefore, adaptive neuro-fuzzy controlled FEES was found to be an effective means for enhancing the transient stability stabilization of the wind generator system network.

IX. Appendix

The data of the IEEE-39 Bus New England test system is provided in Tables III-V.

References

[1] Global Wind Energy Council (GWEC), "Wind is a global power source," *Global Trend-GWEC*, online: http://www.gwec.net, Jan 2013.

[2] Strategic Energy Technology Information Systems (SETIS), "Wind Energy Generation", *European Commission for Wind Energy Generation*, March 2014, online: setis.ec.europa.eu/system/files/Setis_magazine_04_2013.pdf

[3] Hasanien, H.M.; Ali, S.Q.; Muyeen, S.M., "Wind generator stability enhancement by using an adaptive artificial neural network-controlled superconducting magnetic energy storage," *15th International Conference on Electrical Machines and Systems (ICEMS)*, pp. 1-6, 21-24 Oct. 2012.

[4] Juanhua Wang; Jiancheng Zhang; Yun Zhong, "Study on a Super Capacitor Energy Storage system for improving the operating stability of Distributed Generation system," *Third International Conference on Electric Utility Deregulation and Restructuring and Power Technologies, DRPT*, pp.2702-2706, 6-9 April 2008.

[5] Khanna, R.; Singh, G.; Nagsarkar, T. K., "Power system stability enhancement with SMES," *International Conference on Power, Signals, Controls and Computation (EPSCICON)*, 2012, pp.1-6, 3-6 Jan. 2012.

[6] S.M. Muyeen, Hany M. Hasanien, Ahmed Al-Durra, "Transient stability enhancement of wind farms connected to a multi-machine power system by using an adaptive ANN-controlled SMES", *Energy Conversion and Management*, Volume 78, February 2014, Pages 412-420.

[7] Wenjuan Du; Haifeng Wang; Liye Xiao; Dunn, R., "Modeling energy storage systems into electric power transmission systems," *Proceedings of the 44th International Universities Power Engineering Conference (UPEC)*, 2009, pp.1-5, 1-4 Sept. 2009.

[8] Soori, P.K.; Shetty, S.C.; Chacko, S., "Application of super capacitor energy storage in microgrid system," *GCC Conference and Exhibition (GCC), 2011 IEEE*, pp.581-584, 19-22 Feb. 2011.

[9] IEEE Task Force on Benchmark Models for Digital Simulation of FACTS and Custom-Power Controllers, T&D Committee, "Detailed modeling of superconducting magnetic energy storage (SMES) system", *IEEE Transactions on Power Delivery*, vol. 21, no. 2, pp. 699-710, April 2006.

[10] Takahashi, R.; Tamura, J., "Frequency control of isolated power system with wind farm by using Flywheel Energy Storage System," *18th International Conference on Electrical Machines, ICEM 2008*, pp.1-6, 6-9 Sept. 2008.

[11] Mohd. Hasan Ali, Bin Wu, and Roger A. Dougal, "An overview of SMES applications in power and energy systems," *IEEE Transactions on Sustainable Energy*, vol. 1, no. 1, pp. 38-47, April 2010.

[12] Akagi, H., and Sato, H.: "Control and performance of a doubly-fed induction machine intended for a flywheel energy storage system", *IEEE Trans. Power Electron*., 2002, 17, (1), pp. 109–116.

[13] Cardenas, R., Pena, R., Asher, G., and Clare, J.: "Control strategies for enhanced power smoothing in wind energy systems using a flywheel driven by a vector-controlled induction machine", *IEEE Trans. Ind. Electron.*, 2001, 48, (3), pp. 625–635.

[14] Borneman, H.J., and Sander, M.: "Conceptual system design of a 5MWh/100 MW superconducting flywheel energy storage plant for power utility applications", *IEEE Trans. Appl. Supercond.*, 1997,7,(2), pp. 398–401.

[15] Weissbach, R.S., Karady, G.G., and Farmer, R.G.: "Dynamic voltage compensation on distribution feeders using flywheel energy storage", *IEEE Trans. Power Deliv.*, 1999, 14, (2), pp. 165–170.

[16] Hebner, R., Beno, J., and Walls, A.: "Flywheel batteries come around again", *IEEE Spectr*., 2002, pp. 46–51.

[17] Rickard Östergård., "Flywheel energy storage a conceptual study", UPTEC ES11 031 Examensarbete 30 hp, Uppsala Universitet., December 2011.

[18] Islam, F.; Hasanien, H.; Al-Durra, A.; Muyeen, S. M., "A new control strategy for smoothing of wind farm output using short-term ahead wind speed prediction and Flywheel energy storage system," *American Control Conference (ACC)*, pp.3026-3031, 27-29 June 2012.

[19] Kairous, D.; Wamkeue, R.; Belmadani, B., "Sliding mode control of DFIG based variable speed WECS with flywheel energy storage," *XIX International Conference on Electrical Machines (ICEM)*, 6-8 Sept, 2010, pp.1-6.

[20] Wei Qiao; Harley, R.G., "Effect of grid-connected DFIG wind turbines on power system transient stability," *Power and Energy Society General Meeting - Conversion and Delivery of Electrical Energy in the 21st Century*, 2008 IEEE, pp.1-7, 20-24 July 2008.

[21] PSCAD Manual, Manitoba Research Center, Canada, 2014.

[22] Hasanien, H.M., "Shuffled frog leaping algorithm-based static synchronous compensator for transient stability improvement of a grid-connected wind farm," *Renewable Power Generation, IET* , vol.8, no.6, pp.722-730, August 2014.

[23] Hasanien, H.M.; Muyeen, S.M., "A Taguchi Approach for Optimum Design of Proportional-Integral Controllers in Cascaded Control Scheme," *IEEE Transactions on Power Systems,*, vol.28, no.2, pp.1636-1644, May 2013.

[24] Hany M. Hasanien, and S. M. Muyeen, "Design Optimization of Controller Parameters used in Variable Speed Wind Energy Conversion System by Genetic Algorithms", *IEEE Transactions on Sustainable Energy*, vol. 3, no. 2, pp. 200-208, April 2012.

[25] Okedu, K.E.; Muyeen, S. M.; Takahashi, R.; Tamura, J., "Comparative study between two protection schemes for DFIG-based wind generator*," International Conference on Electrical Machines and Systems (ICEMS)*, 2010, pp.62-67, 10-13 Oct. 2010.

[26] G. Li, S. Cheng, J. Wen, Y. Pan and J. Ma, "Power System Stability Enhancement by a Double-fed Induction Machine with a Flywheel Energy Storage System," *IEEE Power Engineering Society General Meeting*, 2006.

[27] Muyeen, S.M.; Hasanien, H.M.; Tamura, J., "Reduction of frequency fluctuation for wind farm connected power systems by an adaptive artificial neural network controlled energy capacitor system," *Renewable Power Generation, IET* , vol.6, no.4, pp.226-235, July 2012.
[28] Rashid, M.H.: 'Power electronics handbook reference book' (Elsevier Inc, 2007, 2nd edn.)
[29] B. Widrow and M. A. Lehr, "30 years of adaptive neural networks: Perceptron, madaline, and backpropagation," in *Proc. IEEE*, vol. 78, pp. 1415-1442, Sept. 1990.
[30] Hany M. Hasanien, "FPGA implementation of adaptive ANN controller for speed regulation of permanent magnet stepper motor drives," *Energy Conversion and Management*, Volume 52, Issue 2, February 2011, Pages 1252-1257.
[31] Hany M. Hasanien, S.M. Muyeen, "Speed control of grid-connected switched reluctance generator driven by variable speed wind turbine using adaptive neural network controller," *Electric Power Systems Research*, Volume 84, Issue 1, March 2012, Pages 206-213.
[32] H. Karimi-Davijani, A. Sheikholeslami, H. Livani and M. Karimi-Davijani "Fuzzy Logic Control of Doubly Fed Induction Generator Wind Turbine'' *World Applied Sciences Journal* 6(4): 499-508,2009.
[33] P. Grabowski, M. Kazmierkowski,B. Bose and F. Blaabjerg, "A simple direct-torque neuro-fuzzy control of PWM-inverter-fed induction motor drive," *IEEE Transactions on Industrial Electronics*, vol. 47, pp. 863-870, 2000.
[34] M. G. Simoes, B. K. Bose and R. J. Spiegel, "Fuzzy logic based intelligent control of a variable speed cage machine wind generation system," *IEEE Transactions on Power Electronics*, vol. 12, pp. 87-95, 1997.
[35] Madbouly, Sayed O.; Soliman, Hussein F.; Hasanien, Hany M.; Badr, M.A, "Fuzzy logic control of brushless doubly fed induction generator," *5th IET International Conference on Power Electronics, Machines and Drives (PEMD 2010)*, pp.1-7, 19-21 April 2010.
[36] Jones, Donald R., Matthias Schonlau, and William J. Welch. "Efficient global optimization of expensive black-box functions." *Journal of Global optimization* 13.4 (1998): 455-492.
[37] Togiti, Varun, "Pattern Recognition of Power System Voltage Stability using Statistical and Algorithmic Methods" (2012). *University of New Orleans Theses and Dissertations*. Paper 1488.
[38] Athay, T.; Podmore, R.; Virmani, S., "A Practical Method for the Direct Analysis of Transient Stability," *IEEE Transactions on Power Apparatus and Systems*, vol.PAS-98, no.2, pp.573-584, March 1979.

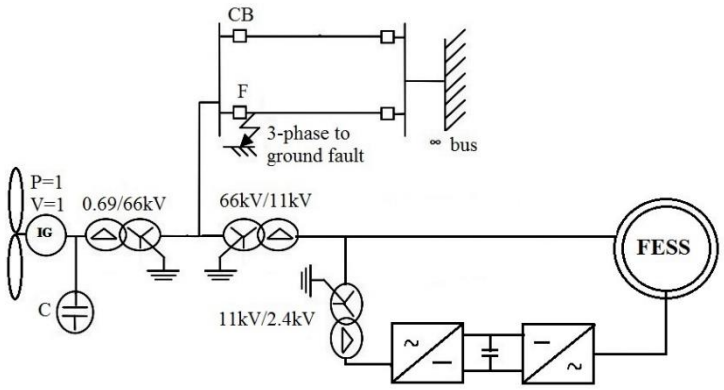

Fig. 1 Model System

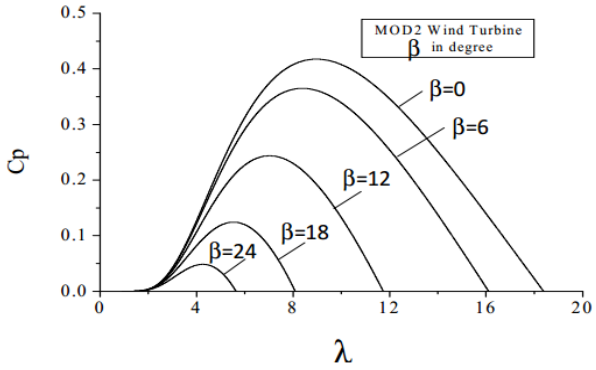

Fig. 2 Cp- λ characteristics for different pitch angles

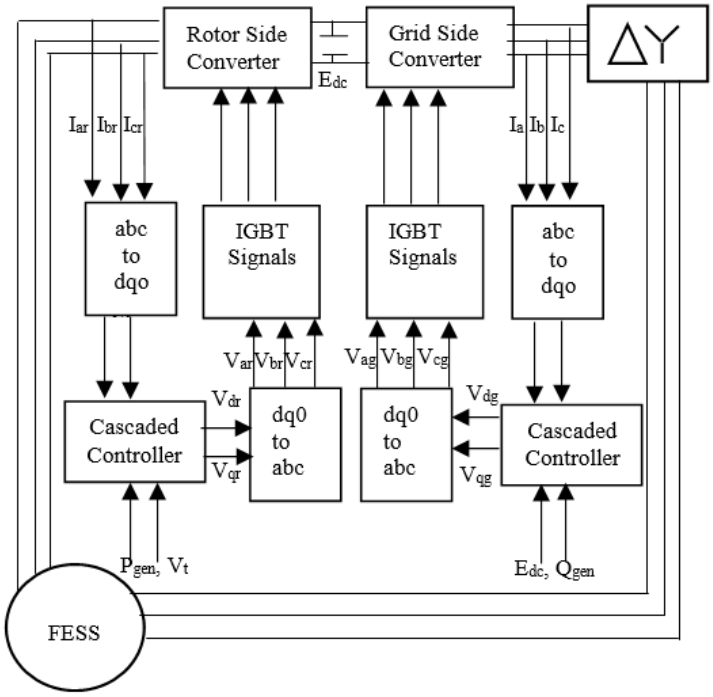

Fig. 3 Model for FESS

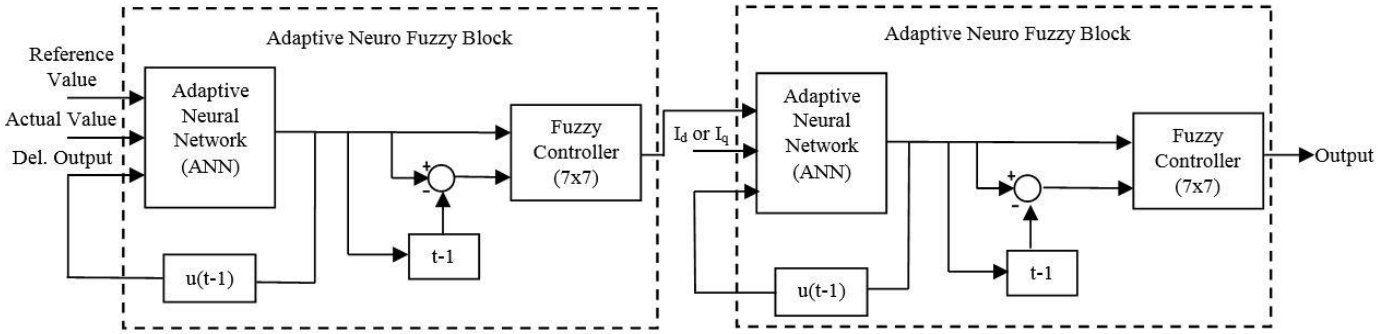

Fig. 4(a) Adaptive neuro fuzzy cascaded control for grid side converter (GSC) and rotor side converter (RSC)

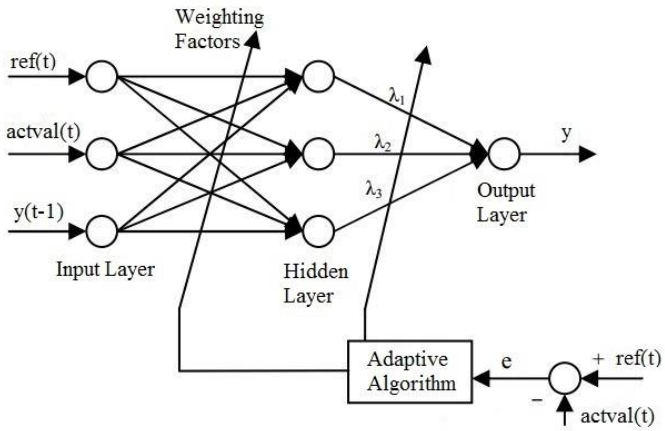

Fig. 4(b) ANN structure

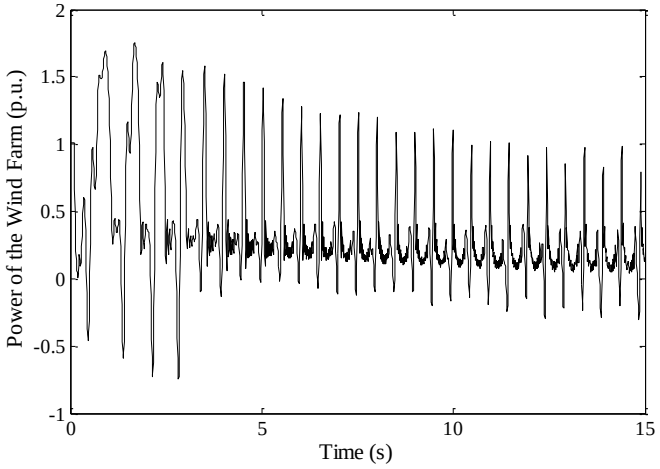
Power of the Wind Farm (p.u.)
2
1.5
1
0.5
0
-0.5
-1
0
5
10
15
Time (s)

(a)

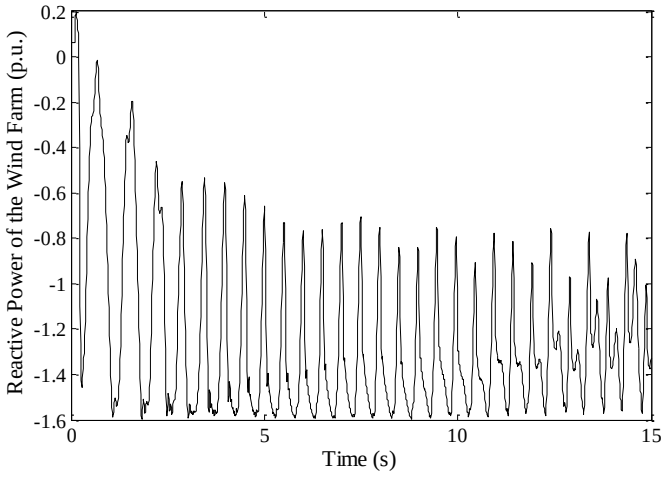
Reactive Power of the Wind Farm (p.u.)
0.2
0
-0.2
-0.4
-0.6
-0.8
-1
-1.2
-1.4
-1.6
0
5
10
15
Time (s)

(b)

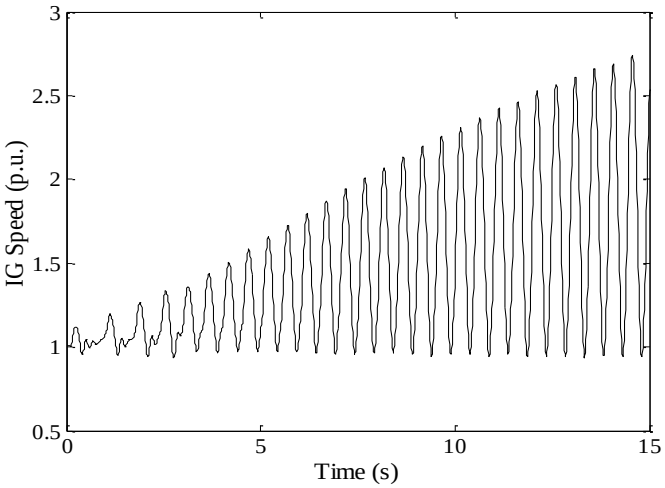
IG Speed (p.u.)
3
2.5
2
1.5
1
0.5
0
5
10
15
Time (s)

(c)

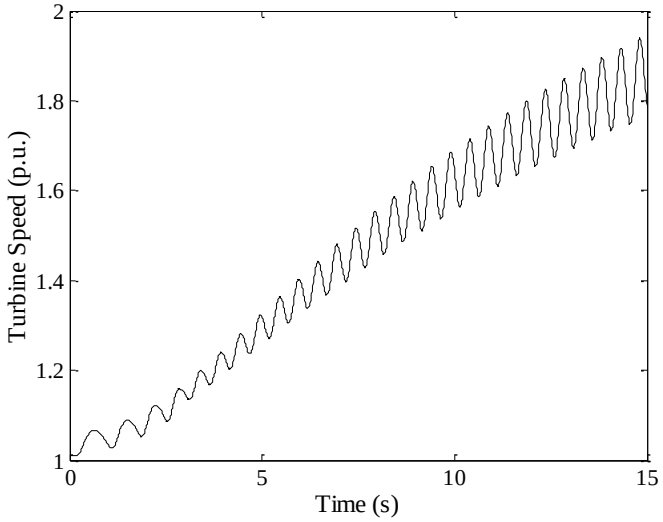

(d)

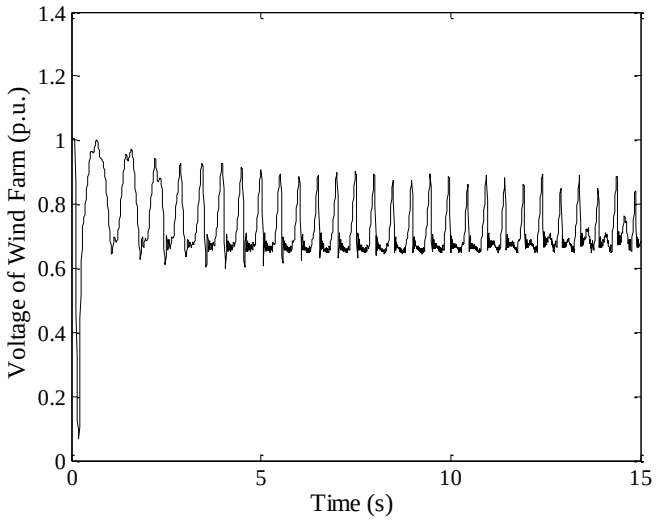

(e)

Fig. 5. System responses without FESS. (a) Active power of the wind farm. (b) Reactive power of the wind farm. (c) IG Speed. (d) Turbine Speed. (e) Voltage of the wind farm.

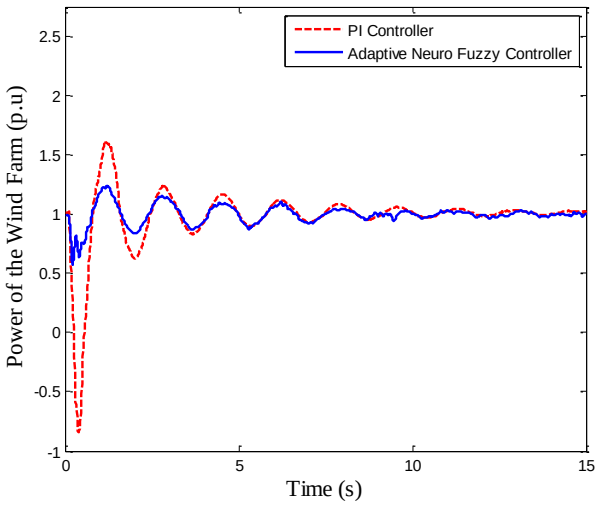

(a)

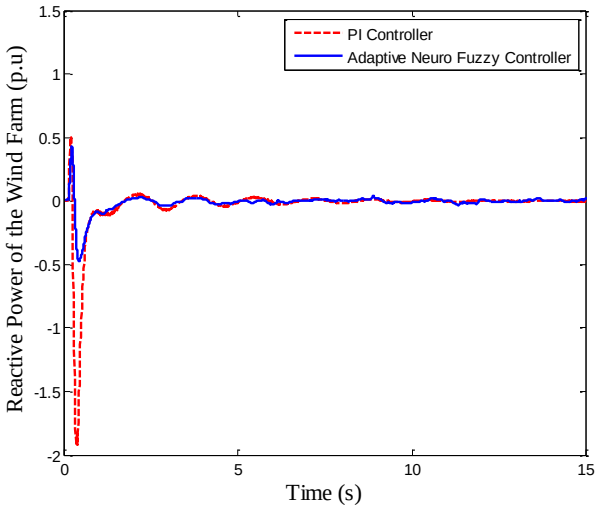
PI Controller
Adaptive Neuro Fuzzy Controller
Reactive Power of the Wind Farm (p.u)
Time (s)

(b)

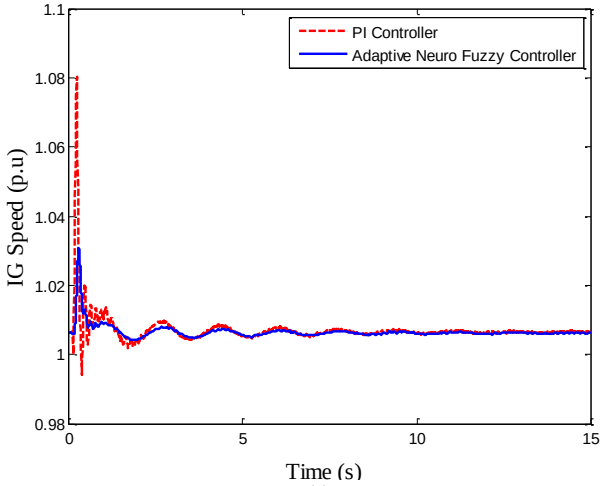
PI Controller
Adaptive Neuro Fuzzy Controller
IG Speed (p.u)
Time (s)

(c)

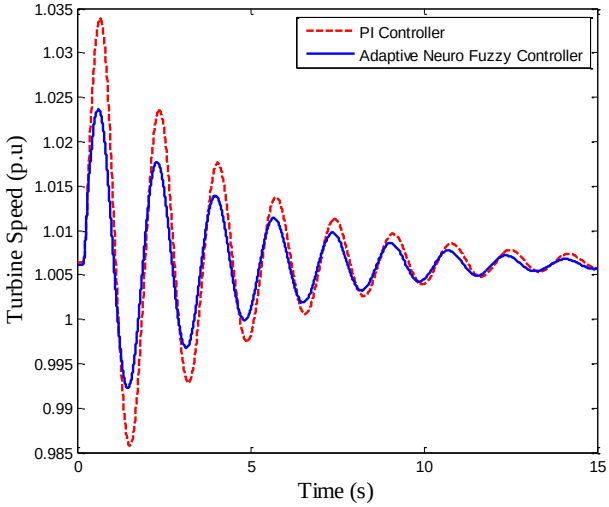
PI Controller
Adaptive Neuro Fuzzy Controller
Turbine Speed (p.u)
Time (s)

(d)

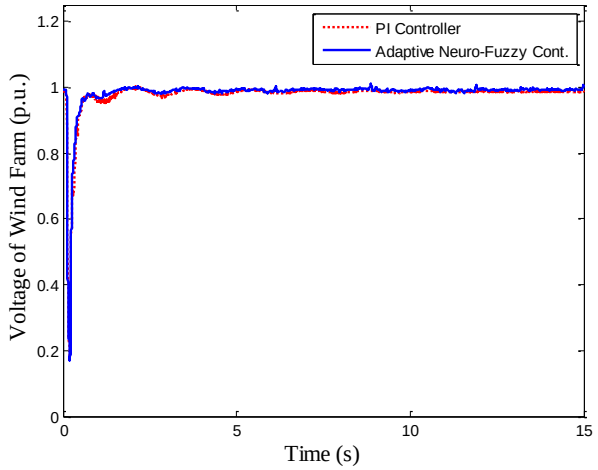

(e)

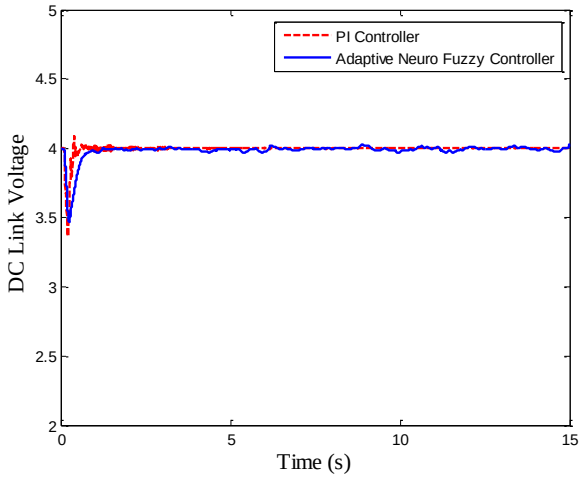

(f)

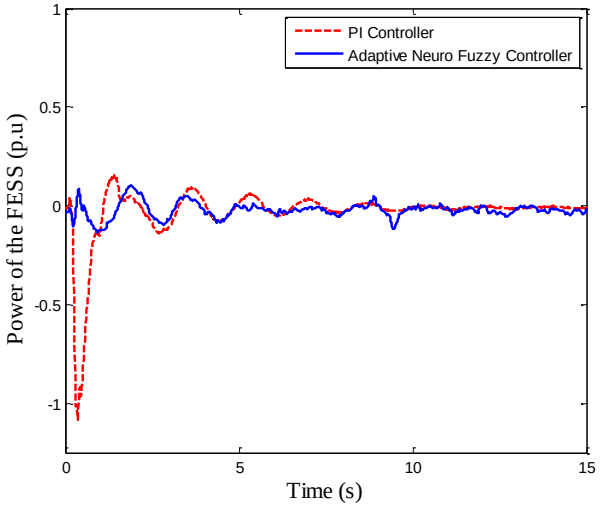

(g)

Fig. 6. System responses with PI and adaptive neuro-fuzzy controlled FESS. (a) Active power of the wind farm. (b) Reactive power of the wind farm. (c) IG Speed. (e) Turbine Speed. (e) Voltage of the wind farm. (f) DC Link voltage (g) Active power of the FESS.

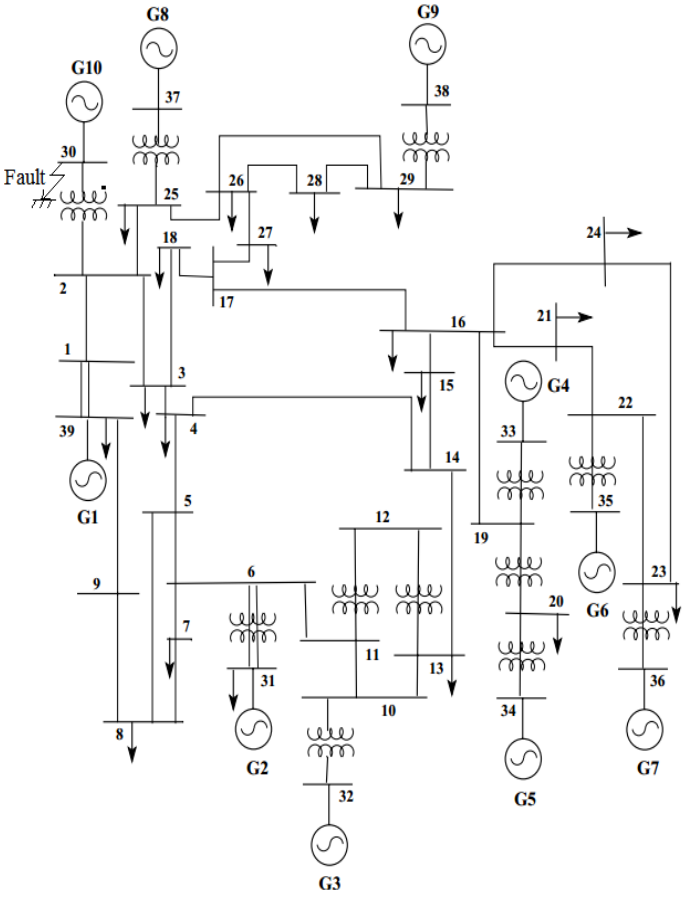

Fig. 7 Single Line Diagram of IEEE-39 Bus New England Test System

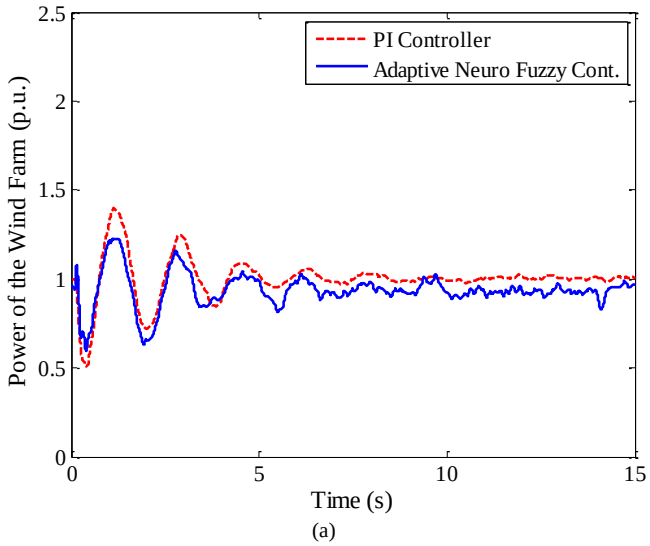

(a)

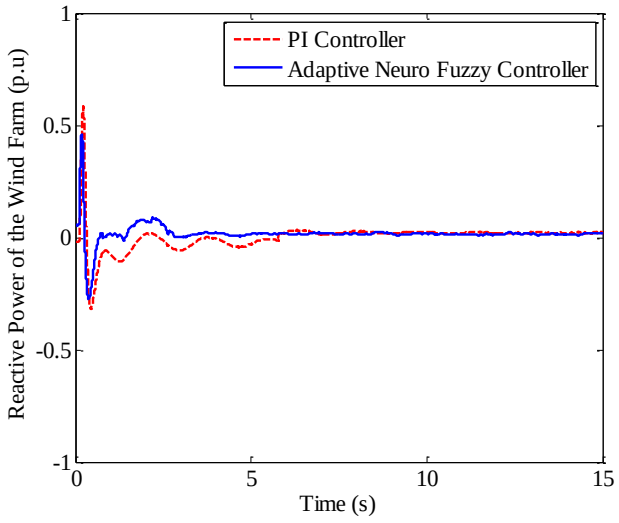
PI Controller
Adaptive Neuro Fuzzy Controller
Reactive Power of the Wind Farm (p.u)
Time (s)
1
0.5
0
-0.5
-1
0
5
10
15

(b)

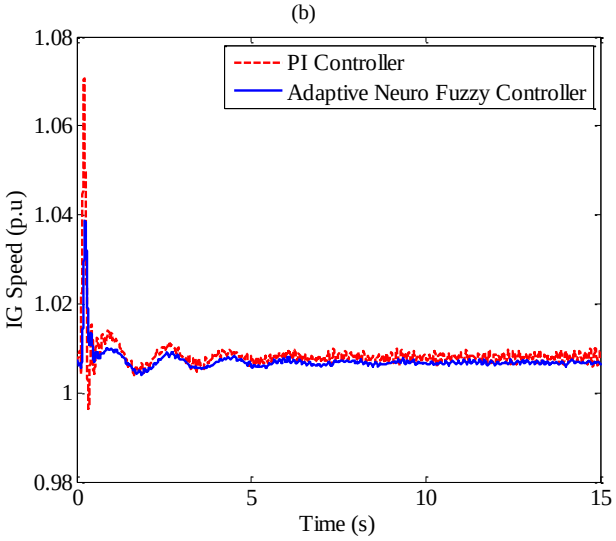
PI Controller
Adaptive Neuro Fuzzy Controller
IG Speed (p.u)
Time (s)
1.08
1.06
1.04
1.02
1
0.98
0
5
10
15

(c)

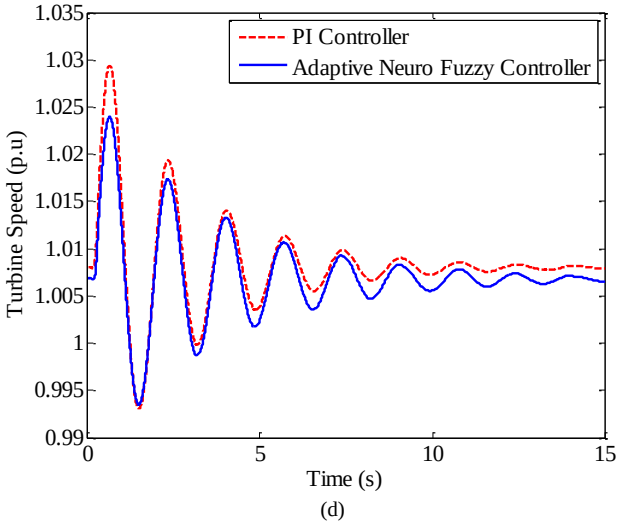
PI Controller
Adaptive Neuro Fuzzy Controller
Turbine Speed (p.u)
Time (s)
1.035
1.03
1.025
1.02
1.015
1.01
1.005
1
0.995
0.99
0
5
10
15

(d)

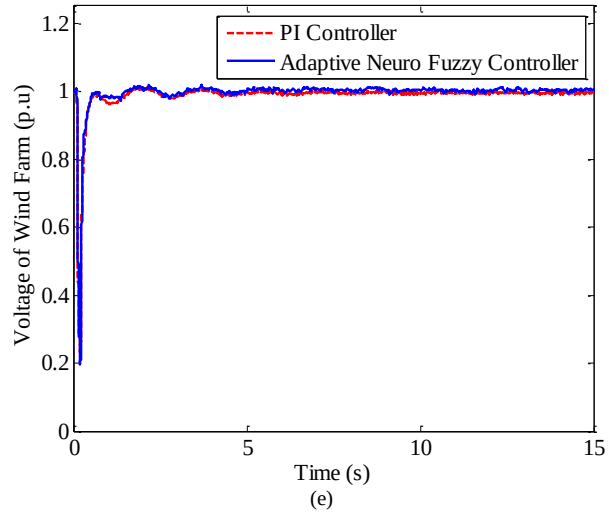

(e)

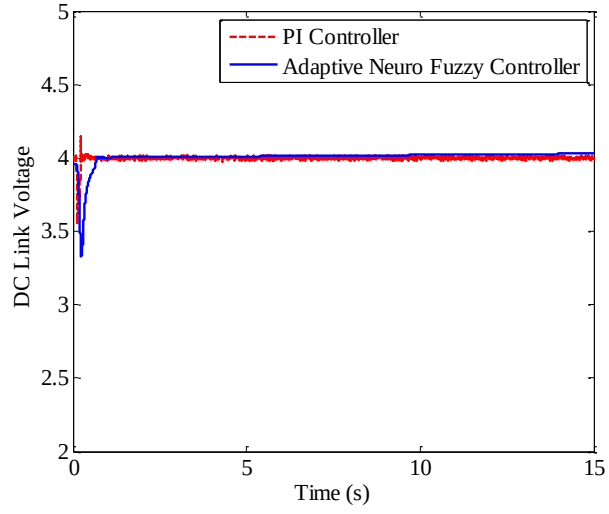

(f)

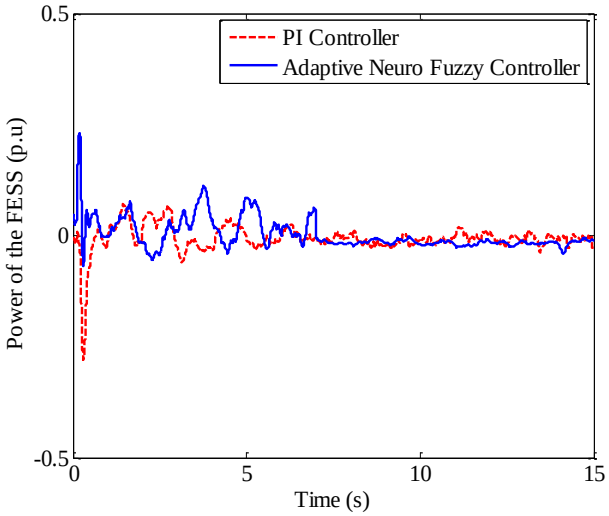

(g)

Fig. 8. System responses with PI and adaptive neuro fuzzy controlled FESS. (a) Active power of the wind farm (b) Reactive power of the wind farm. (c) IG Speed. (e) Turbine Speed. (e) Voltage of the wind farm. (f) DC Link voltage. (g) Active power of the FESS.

Table I
IG AND FESS Parameters

	Induction Generator (IG)	FESS
Stator resistance (p.u)	0.01	0.01
Stator leakage reactance (p.u)	0.1	0.05
Rotor resistance (p.u)	0.01	0.007
Rotor leakage reactance (p.u)	0.12	0.05
Magnetizing reactance (p.u)	3.5	4.01
Inertia Constant H (s)	1.5	15

Table II
Decision Table for 7x7 FLC

	NL	NM	NS	Z	PS	PM	PL
NL	NL	NB	NB	NM	NS	NS	Z
NM	NL	NM	NM	NM	NS	Z	PS
NS	NL	NM	NS	NS	Z	PS	PM
Z	NL	NM	NS	Z	PS	PM	PL
PS	NM	NS	Z	PS	PS	PM	PL
PM	NS	Z	PS	PM	PM	PM	PL
PL	Z	PS	PS	PM	PL	PL	PL

Table III
Generator Data for IEEE 39 Bus System

Bus	Generator Total Power (MVA)	Pgen (MW)	Voltage of the Bus (p.u)
30	1290	250	1.0475
31	574	520.81	0.982
32	753	650	0.9831
33	917	632	0.9972
34	303	508	1.0123
35	800	650	1.0493
36	816	560	1.0635
37	702	540	1.0278
38	702	830	1.0265
39	6667	1000	1.03

Table IV
Bus Data for IEEE 39 Bus System

Bus	Bus Name	Base kV	Voltage (p.u)	Angle (deg.)
1	Bus 1	345	1.045	-8.54
2	Bus 2	345	1.041	-5.82
3	Bus 3	345	1.025	-8.68
4	Bus 4	345	1.001	-9.68
5	Bus 5	345	1.003	-8.67
6	Bus 6	345	1.006	-8.01
7	Bus 7	345	0.995	-10.19
8	Bus 8	345	0.994	-10.69
9	Bus 9	345	1.028	-10.41
10	Bus 10	345	1.015	-5.48
11	Bus 11	345	1.011	-6.34
12	Bus 12	345	0.998	-6.31
13	Bus 13	345	1.012	-6.16
14	Bus 14	345	1.009	-7.72
15	Bus 15	345	1.013	-7.79
16	Bus 16	345	1.029	-6.23
17	Bus 17	345	1.03	-7.34
18	Bus 18	345	1.027	-8.28
19	Bus 19	345	1.049	-1.06
20	Bus 20	345	0.991	-2.05
21	Bus 21	345	1.03	-3.82
22	Bus 22	345	1.049	0.64
23	Bus 23	345	1.044	0.44
24	Bus 24	345	1.035	-6.11
25	Bus 25	345	1.044	-4.18
26	Bus 26	345	1.045	-5.47
27	Bus 27	345	1.032	-7.49
28	Bus 28	345	1.047	-1.93
29	Bus 29	345	1.048	0.84
30	Gen 10	22	1.048	-3.39
31	Gen 2	22	0.982	0
32	Gen 3	22	0.983	2.51
33	Gen 4	22	0.997	4.16
34	Gen 5	22	1.012	3.14
35	Gen 6	22	1.049	5.59
36	Gen 7	22	1.064	8.3
37	Gen 8	22	1.028	2.51
38	Gen 9	22	1.027	7.91
39	Gen 1	345	1.03	-10.15

Table V
Load Data for IEEE-39 Bus System

Bus Number	Pload (MW)	Qload (Mvar)
3	322	2.4
4	500	184
7	233.8	84
8	522	176
12	8.5	88
15	320	153
16	329	32.3
18	158	30
20	628	103
21	274	115
23	247.5	84.6
24	308.6	-92
25	224	47.2
26	139	17
27	281	75.5
28	206	27.6
29	283.5	26.9
31	9.2	4.6
39	1104	250